



## Research Article

# DESIGN, CHARACTERIZATION, AND EVALUATION OF AN ACECLOFENAC COCRYSTAL FOR IMPROVED SOLUBILITY AND STABILITY

Aditay Kumar, Mahesh Kumar\*

### Article Information

Received: 18<sup>th</sup> August 2025  
Revised: 15<sup>th</sup> October 2025  
Accepted: 11<sup>th</sup> November 2025  
Published: 25<sup>th</sup> December 2025

### Keywords

Pharmaceutical cocrystal,  
Aceclofenac, Solubility, *In vivo*,  
*In vitro*, Stability study

### ABSTRACT

**Background:** Co-crystallization enhances APIs by forming noncovalent interactions with cofomers, thereby improving physicochemical properties. Aceclofenac was selected for its low solubility, whereas L-lysine serves as a cofomer to enhance solubility and stability via hydrogen bonding. This strategy effectively improves the solubility, stability, and bioavailability of poorly soluble drugs. **Methods:** The aceclofenac–lysine co-crystal was synthesized using the Neat Grinding technique. The synthesized cocrystal was characterized by powder X-ray diffraction (PXRD), differential scanning calorimetry (DSC), Hot stage microscopy (HSM), and Fourier transform infrared spectroscopy (FTIR). Dissolution behavior, stability, and *in vivo* anti-inflammatory activity were evaluated in comparison with pure aceclofenac. **Results:** PXRD and DSC confirmed a new crystalline phase, while FTIR revealed hydrogen bonding between aceclofenac and lysine. The cocrystal exhibited a 2.66-fold improvement in dissolution (91.84% vs. 34.41% at 90 min) and superior stability, maintaining >86% dissolution after six months at 40°C/75% RH, compared to ~30% for pure aceclofenac. *In vivo* studies demonstrated enhanced anti-inflammatory efficacy, with 81.50% edema inhibition versus 74.35% with the pure drug ( $p < 0.0001$ ). **Discussion:** The ACF-lysine cocrystal achieved dissolution enhancement that maintained stability over six months, and demonstrated statistically significant improvement in anti-inflammatory efficacy, confirming superior therapeutic performance over pure aceclofenac. **Conclusion:** Co-crystallization with L-lysine effectively enhanced aceclofenac's biopharmaceutical and pharmacological performance. The aceclofenac-lysine co-crystal exhibited 2.66-fold faster dissolution, greater stability under accelerated storage, and significantly improved anti-inflammatory efficacy (81.50% vs. 74.35% edema inhibition;  $p < 0.0001$ ) compared with pure aceclofenac. These results demonstrate the value of amino acid cofomers in improving the solubility of poorly soluble drugs.

### INTRODUCTION

Aceclofenac (ACF) is a nonsteroidal anti-inflammatory drug (NSAID) commonly used to treat chronic musculoskeletal

conditions, including osteoarthritis, ankylosing spondylitis, and rheumatoid arthritis. It exerts anti-inflammatory, analgesic, and antipyretic effects primarily by selectively inhibiting

\*Department of Pharmaceutical Sciences, MDU Rohtak, Haryana, India, 124001

\*For Correspondence: [drmaheshmdu22@gmail.com](mailto:drmaheshmdu22@gmail.com)

©2025 The authors

This is an Open Access article distributed under the terms of the Creative Commons Attribution (CC BY NC), which permits unrestricted use, distribution, and reproduction in any medium, as long as the original authors and source are cited. No permission is required from the authors or the publishers. (<https://creativecommons.org/licenses/by-nc/4.0/>)

cyclooxygenase-2 (COX-2), with better gastrointestinal tolerability than conventional NSAIDs such as diclofenac and naproxen [1]. According to the Biopharmaceutical Classification System (BCS), aceclofenac (ACF) is classified as Class II, characterized by high permeability and low aqueous solubility, with reported water solubility of  $\sim 60 \mu\text{g/mL}$  at  $25^\circ\text{C}$  [1, 2]. The presence of a carboxylic acid group ( $\text{pK}_a \sim 4.7$ ) provides a reliable proton donor site, while additional acceptor groups (carbonyl and ether oxygens) enable robust hydrogen-bonding networks with suitable coformers [3]. Its aromatic rings and ether linkage further support  $\pi$ - $\pi$  stacking and van der Waals interactions, which favor stable lattice formation [3]. With a melting point of  $154\text{--}158^\circ\text{C}$ , the compound has manageable thermal stability for crystallization, and its moderate lipophilicity ( $\text{LogP } 2.7\text{--}3.0$ ) allows flexibility in selecting both hydrophilic and hydrophobic coformers [1]. Together, these features indicate that cocrystallization can enhance solubility and dissolution rate without altering the drug's pharmacological activity, making aceclofenac a rational choice for pharmaceutical cocrystal design [4]. Nonetheless, solid dispersion systems pose challenges related to physical stability and to environmental temperature and humidity, which can alter crystallinity and, consequently, dissolution performance [5]. While the cyclodextrins used in inclusion complexes are generally considered safe, their high doses pose a risk of nephrotoxicity [6].

Multicomponent crystal (MCC) formation, including cocrystals, salts, and solvates, represents a promising strategy to enhance aceclofenac's solubility, dissolution rate, and stability while preserving therapeutic efficacy [7–9]. Several ACF cocrystals with amino acids and nicotinamide have demonstrated significant dissolution improvements [8, 9]. According to the U.S. Food and Drug Administration (FDA), pharmaceutical cocrystals are crystalline solids comprising an active pharmaceutical ingredient (API) and one or more coformers arranged within the same crystal lattice [10]. Nonionic, noncovalent interactions link the molecular components, distinguishing cocrystals from salts or polymorphs. Typically, a cocrystal comprises an active pharmaceutical ingredient (API) and a coformer used to form the cocrystal. Cocrystals and solvates differ fundamentally in composition: solvates incorporate solvent molecules into the crystal lattice alongside the API. In contrast, cocrystals consist of the API and one or more solid coformers in a defined stoichiometric ratio. Both typically exist as crystalline solids at room temperature. In

solvates, solvent molecules occupy specific lattice positions without forming covalent bonds, thereby influencing the solid's physicochemical properties. Hydrates, a subclass of solvates that contain water molecules, are crystalline solids whose water content affects drug stability, solubility, and dissolution characteristics [11–12]. Coformers selected for the preparation of pharmaceutical cocrystals should be classified as Generally Recognized as Safe (GRAS) by the U.S. Food and Drug Administration to ensure their suitability for human health applications. [13–14]. Various coformers are used in the preparation of pharmaceutical cocrystals, such as maleic acid, L-lysine, malic acid, and Malonic acid, as shown in **Figure 1**.

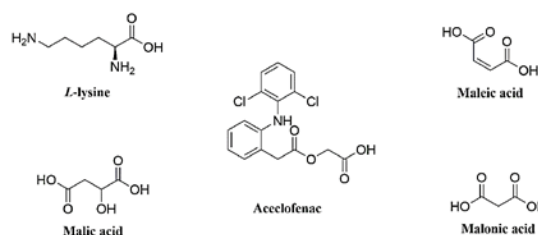


**Figure 1: Chemical structure of ACF and various Coformers**  
 Aceclofenac (ACF) has been co-crystallized with a range of coformers, including urea, N, N-dimethylurea, L-cystine, nicotinamide, nicotinic acid, gallic acid, chitosan, and caffeine, highlighting the ability of co-crystallization to enhance its physicochemical properties, such as solubility and stability [15–18].

#### MATERIALS AND METHODS

Aceclofenac (ACF) and L-lysine were obtained from CDH, Mumbai, India. Ethanol (analytical grade) was purchased from RANKEM Chemicals, India. All other reagents and excipients, including buffers, salts, and coformers, were of analytical grade and used as received. Ultra-purified water (resistivity  $18.2 \text{ M}\Omega\cdot\text{cm}$ , Milli-Q system, Merck Millipore, India) was employed throughout the experiments. To protect ACF from light-induced degradation, all procedures were carried out in dark amber glass containers.

#### Screening and Selection of the Coformer

The drug Aceclofenac was selected for this study due to its low aqueous solubility and limited bioavailability, making it a suitable candidate for cocrystallization to enhance its physicochemical properties. Choosing an appropriate coformer is a crucial step in cocrystal development. Several approaches can be used for this purpose, including lattice energy calculations, evaluation of intramolecular hydrogen bonding,  $\text{pK}_a$ -based models, analysis of supramolecular synthons using the Cambridge Structural Database (CSD), and assessment of

Hansen solubility parameters. Out of these approaches, a virtual cocrystal screening method based on Molecular Electrostatic Surface Potentials (MESP) was adopted to refine the selection process and reduce experimental workload. Based on this analysis, L-lysine was identified as a suitable coformer due to its complementary functional groups that can form strong hydrogen bonds and enhance solubility. L-lysine was selected over other GRAS coformers (maleic, malic, and malonic acids) based on its exceptionally high interaction energy (37.6 kJ/mol vs. 18.5-25.7 kJ/mol), unique zwitterionic character enabling multiple hydrogen-bonding modes, superior electrostatic complementarity with aceclofenac functional groups, and established pharmaceutical safety profile. Computational predictions were validated experimentally: only L-lysine formed stable cocrystals, whereas other coformers failed despite computational screening, thereby confirming the reliability of MESP-based selection criteria. This systematic approach improved the reliability of coformer selection while minimizing the number of experimental trials required [19].

### Computational Details

For virtual screening, the molecular geometries of ACF and the selected coformers were optimized using ORCA, employing the M06-2X functional with the 6-311++G(d,p) basis set. The molecular electrostatic potential (MESP) maxima and minima were then determined using Multiwfn version 3.8, based on the optimized structures, with an isosurface value set at 0.002 Bohr  $\text{\AA}^{-3}$  [22]. The methodology aims to identify potential hydrogen-bonding sites and predict cocrystal formation by calculating molecular electrostatic surface potentials (MESP).

**Methodology:** For each molecule:

- Optimize molecular geometry using DFT at M062X/6-311++G(d,p) level of theory
- Extract MESP maxima (electron-poor regions, hydrogen bond donors) and minima (electron-rich regions, hydrogen bond acceptors).

The transformed H-bond parameters (donor  $\alpha$  and acceptor  $\beta$ ) were calculated from MESP maxima and minima using equations 1 and 2, respectively [21].

$$\alpha = 0.0000162 \text{ MEP max2} + 0.00962 \text{ MEP max}''$$

$$\beta = 0.000146 \text{ MEP min2} - 0.00930 \text{ MEP min}''$$

- Determine the injection energy (E) from the strongest donors in combination with the strongest acceptors. By assembling the best  $\alpha$  with the best  $\beta$  in a hierarchical order, the solid E can be estimated approximately.

$$E = - \sum_{ij} \alpha_i \beta_j$$

- $\Delta E$  can do estimation of cocrystal formation. Within this approximation, one calculates the difference of the cocrystal pairing energies  $E_{\text{cocrystal}}$  with those of the pure components  $E_{\text{API}}$  and  $E_{\text{coformer}}$ .

$$\Delta E = E_{\text{cocrystal}} - E_{\text{API}} - E_{\text{coformer}}$$

- With the above approach,  $\Delta E > 11$  kJ/mol is set as an estimate for the energy threshold that defines a probability of cocrystal formation. Although this method has limitations, it is efficient and straightforward to apply when screening large numbers of coformer molecules.

### Preparation of ACF-LYS Cocrystal

The cocrystal comprising aceclofenac (ACF) and L-lysine (LYS) was prepared using a Neat Grinding method, a solvent-free approach consistent with green chemistry principles. Equimolar amounts of ACF and LYS (1:1 molar ratio) were accurately weighed and mixed in a clean, dry mortar. Manual grinding was performed using a pestle for approximately 45 minutes at room temperature to promote solid-state interactions between the API and coformer. The grinding process was continued until a homogeneous fine powder was obtained. Formation of the new solid phase was monitored by periodic powder X-ray diffraction (PXRD) and differential scanning calorimetry (DSC), which revealed distinct diffraction peaks and thermal transitions that differed from those of the parent compounds and their physical mixture, indicating successful cocrystal formation rather than a polymorphic or solvate form. No evidence of degradation was observed, as verified by comparing the FTIR spectra and PXRD patterns with those of pure ACF and LYS. Alternative preparation methods, including solvent-assisted grinding and solution crystallization, were considered; however, neat grinding was selected for its simplicity, reproducibility, and elimination of solvent-related impurities. The propensity for single-crystal formation was not observed under these conditions, likely due to the kinetics of solid-state grinding; the product remained a microcrystalline powder suitable for solid-state characterization.

### Characterization of ACF-LYS Cocrystal Differential scanning calorimetry

Thermal analysis was performed using a DSC Q10 V9.9 instrument (TA Instruments, USA). The instrument was first calibrated using an indium standard to ensure precise melting-point measurements. For each analysis, 3–5 mg of sample, pure aceclofenac, and prepared cocrystal were placed in a T-zero

aluminum pan. The samples were heated from 40 °C to 200 °C at 10 °C/min under a nitrogen flow rate of 60 mL/min. Thermograms were recorded and examined to determine melting points and other thermal transitions, thereby confirming the formation of the cocrystal [23].

### HSM

Hot-stage microscopy (HSM) was performed using a Linkam THMS600 hot stage attached to an Olympus microscope. Data acquisition and temperature control were managed using LINK software integrated with the Linksys32 module, enabling precise regulation of the hot stage.

### Fourier transform IR (FTIR)

Fourier-transform infrared (FTIR) spectra were obtained using an Alpha Bruker spectrometer (Model 120,602,880; Bruker, Germany). Measurements were carried out over the range of 4000–400  $\text{cm}^{-1}$  with a resolution of 4  $\text{cm}^{-1}$ . Each spectrum represented the average of 32 scans to improve accuracy and reduce background noise. The samples were analyzed using attenuated total reflectance technique. Data collection and interpretation were performed using OPUS software (Bruker).

### Powder X-ray diffraction (PXRD)

Powder X-ray diffraction (PXRD) analysis was performed to characterize the crystalline phases of the samples. The measurements were carried out on a PANalytical X'Pert PRO diffractometer (PANalytical, Netherlands) operating with Cu K $\alpha$  radiation ( $\lambda = 1.54060 \text{ \AA}$ ). Before analysis, the instrument was calibrated using a silicon standard to ensure accurate peak positions. Data were collected over a  $2\theta$  range of 3.5°–50°, with a step size of 0.017° and a counting time of 25 seconds per step. The obtained diffraction profiles were compared with reference patterns of the pure components and their physical mixture to confirm the formation of a new solid phase. Diffraction data were processed and interpreted using X'Pert HighScore software (PANalytical), which enabled phase identification and evaluation of structural differences between the cocrystal and its parent materials [24].

### Dissolution Studies

*In vitro* studies performed revolved around assessing the release kinetics associated with pure aceclofenac (ACF) and its derivatives, which included a synthesized ACF-lysine cocrystal, physical mixture (ACF with cofomer), as well as a commercial formulation, Zerodol (IPCA). The dissolution study was conducted using a USP Type II (paddle) apparatus (Lab

India DS8000, Lab India Analytical, Maharashtra, India). The test was performed in 900 mL of phosphate buffer (pH 7.5) maintained at  $37 \pm 0.5 \text{ }^\circ\text{C}$ , with a paddle rotation speed of 50 rpm to simulate physiological conditions. Sampling was carried out at predefined time intervals by withdrawing 5 mL aliquots from the dissolution medium. To maintain sink conditions and constant volume, each withdrawn sample was immediately replaced with an equal volume (5 mL) of fresh phosphate buffer (pH 7.5). Spectrophotometric analysis was conducted on all samples post-0.45  $\mu\text{m}$  filtration at  $\lambda_{\text{max}}$  276 nm using a Shimadzu UV-800 spectrophotometer. All experiments were performed in triplicate, and the reported data are presented as mean  $\pm$  standard deviation ( $n = 3$ ).

### *In vivo* studies

The *in vivo* studies were conducted after Institutional Animal Ethical Committee permission via letter CAH/2023/46-60 dated 02/03/2023. For this, 20 Wistar rats with an average weight of 190–250g were obtained from the Central Animal House at Maharshi Dayanand University, Rohtak (Reg. No. 1767GO/RE/S/14/CPCSEA dated 18/07/2014 and renewed on 06/10/2022).

All procedures adhered to current standards for the care and use of laboratory animals and to ethical protocols. The animals were given free access to water and food; however, Wistar rats fasted for 12 hours and had unrestricted access to water before the experiments to prevent undue stress and adverse health effects, which can compromise their well-being and the validity of the research outcomes. The pharmaceutical cocrystal was evaluated for anti-inflammatory activity in rats through the carrageenan-induced paw oedema method.

### Human and animal rights

CPCSEA guidelines (New Delhi) were strictly followed for animal experimental procedures. All reported methods aligned with these established standards.

### Anti-inflammatory activity

The anti-inflammatory response of the drug's pure form and the optimized cocrystals was assessed using the carrageenan-induced rat paw edema model, as previously reported (Kulkarni, 1997). Using random selection, adult male Wistar rats ( $n = 20$ ) were assigned to 4 experimental groups, each with 5 animals. All subjects fasted for 12 hours before the initiation of the experiment. In group I (control group), subjects received a carrageenan injection (0.05 mL of 1% solution) but received no other treatment. Group II (vehicle control) received an oral dose

of 1 mL of 0.5% sodium carboxymethyl cellulose (CMC), while Group III (test group) received aceclofenac at 10 mg/kg, suspended in 0.5% CMC. Group IV received cocrystals containing an equivalent dose of aceclofenac 10 mg/kg [25]. All subjects fasted for 12 hours before treatment. After 30 minutes of treatment, inflammation was triggered in all subjects through the subcutaneous injection of 0.05 mL of 1% carrageenan solution in saline solution containing normal saline 0.05 mL at the paw's plantar side of the left hind limb. The plethysmometer was used to quantify paw volume immediately before carrageenan administration (baseline measurement) and at 1-hour intervals for 5 hours post-inflammation to capture inflammation progression. The % of edema reduction was determined for each group at each time point using the formula:

$$\% \text{ Inhibition} = \frac{\text{Mean paw volume of (control)} - \text{mean paw volume (treated)}}{\text{mean paw volume (control)}} \times 100$$

## RESULTS AND DISCUSSION

### Molecular Modelling screening

Cofomer selection was refined using a molecular modelling approach based on molecular electrostatic surface potential (MESP) analysis. The workflow consisted of: (i) optimization of the molecular structures of aceclofenac (ACF) and potential cofomers; (ii) generation of MESP maps to highlight possible

donor and acceptor sites; (iii) calculation of interaction energies ( $\Delta E$ ) between ACF and each cofomer; and (iv) selection of candidates with favorable complementarity. The shortlisted cofomers were then verified experimentally using differential scanning calorimetry (DSC), hot-stage microscopy (HSM), and solid-state preparation of the cocrystals. This combined computational–experimental approach reduced unnecessary experimental trials and provided a more systematic approach to cofomer selection. The results of molecular modelling for the drug and various cofomers are presented in Table 1. Based on the MESP results, L-lysine showed the highest positive potential at the  $\text{NH}_3^+$  site ( $+120.4 \text{ kJ mol}^{-1}$ ) and the most negative potential at the  $\text{COO}^-$  site ( $-78.2 \text{ kJ mol}^{-1}$ ), indicating strong donor-acceptor complementarity with aceclofenac's carboxylic and amide groups. This suggested a high probability of forming stable hydrogen-bond networks. Interaction energies ( $\Delta E$ ) were further calculated to quantify these observations, as summarized in Table 2. In computational cocrystal screening,  $\Delta E$  represents the calculated interaction energy between the drug and cofomer. A  $\Delta E$  above a set threshold, such as 11 kJ/mol, indicates a roughly 50% probability of stable cocrystal formation (Table 2). This method enables rapid, straightforward screening of multiple cofomers. However, it has limitations, including the neglect of solvent effects and kinetic factors.

**Table 1: MESP Values (kJ/mol) of different cofomers and drug**

Molecule	Site	MESP Maxima ( $\alpha$ , kJ mol <sup>-1</sup> )	MESP Minima ( $\beta$ , kJ mol <sup>-1</sup> )
Aceclofenac	O-H (carboxylic)	+85.2	-
	N-H (amide)	+45.8	-
	C=O (carboxylic)	-	-74.6
	C=O (amide)	-	-68.3
	Cl	-	-42.7
Lysine	$\text{NH}_3^+$	+120.4	-
	$\text{NH}_2$	+65.8	-
	$\text{COO}^-$	-	-78.2
	$\text{NH}_2$	-	-52.6
Maleic Acid	O-H	+98.7	-
	C=O	-	-76.3
	C=C	-	-42.8
Malic Acid	O-H (carboxylic)	+95.2	-
	O-H (hydroxyl)	+76.3	-
	C=O	-	-74.9
	O-H (hydroxyl)	-	-58.4
Malonic Acid	O-H	+92.6	-
	C=O	-	-72.5

**Table 2: Correlation between computational predictions and experimental outcomes for ACF cocrystallization**

Cofomers	Donor-Acceptor Pair	Computational		Experimental	Dissolution	Prediction
		Energy (kJ/mol)	$\Delta E$ (kJ/mol)	DSC Outcome		
Lysine	NH <sub>3</sub> <sup>+</sup> (Lysine)···C=O (Aceclofenac carboxylic)	-4.28	37.6	Single Peak (match)	91.84	Cocrystal
	O-H (Aceclofenac)···COO <sup>-</sup> (Lysine)	-2.96				
	N-H (Aceclofenac)···Pyridine N	-1.74				
Maleic Acid	O-H (Maleic)···C=O (Aceclofenac carboxylic)	-3.45	25.7	Two Peaks	NA	No cocrystals
	O-H (Aceclofenac)···C=O (Maleic)	-2.84				
Malic Acid	O-H (Malic) carboxylic···C=O (Aceclofenac carboxylic)	-3.19	22.3	Two Peaks	NA	No cocrystals
	O-H (Aceclofenac)···C=O (Malic)	-2.77				
Malonic Acid	O-H (Malonic)···C=O (Aceclofenac carboxylic)	-2.99	18.5	Two Peaks	NA	No cocrystals
	O-H (Aceclofenac)···C=O (Malonic)	-2.66				

Specifically,  $\alpha$  (MESP maxima) and  $\beta$  (MESP minima) represent the positive and negative regions of the molecular electrostatic surface potential, corresponding to hydrogen-bond donor and acceptor sites, respectively. All values are expressed in kilojoules per mole (kJ mol<sup>-1</sup>). The interaction energy ( $\Delta E$ ) between aceclofenac and each cofomer was calculated using:  $\Delta E = E_{\text{complex}} - (E_{\text{drug}} + E_{\text{coformer}})$ . The  $\Delta E$  results confirm that L-lysine exhibits the strongest interaction energy (37.6 kJ mol<sup>-1</sup>) compared with other cofomers such as maleic, malic, and malonic acids, which showed lower  $\Delta E$  values (18–25 kJ mol<sup>-1</sup>). These findings support the conclusion that L-lysine exhibits superior electrostatic complementarity and interaction strength with aceclofenac, thereby justifying its selection for experimental cocrystallization. Furthermore, the correlation between computed  $\Delta E$  values and observed experimental outcomes validates the reliability of the computational screening approach. Despite a modest success rate, the virtual screen described above provides a reasonable indication of cofomer candidates for experimental screening from a large pool of cofomers. The above virtual screening method ignores structural implications. It is worth noting that the preparation of some cocrystals requires high activation energy [26]; thus, unsuccessful attempts using conventional preparation methods may yield positive results when prepared by kinetically driven processes such as spray drying [27].

### Thermal studies

Differential scanning calorimetry (DSC) of pure aceclofenac (ACF) revealed a sharp endothermic peak at approximately 156

°C, consistent with its reported melting range of 149–158 °C [24]. L-lysine (LYS), used as a cofomer, exhibited a melting transition near 218 °C [24]. The synthesized ACF-LYS cocrystal displayed a distinctive melting endotherm at 205 °C, positioned between the melting points of the two parent components. The Hot-stage microscopy (HSM) observations supported these findings: the cocrystal began to melt at 203.6 °C and completely melted at 206.8 °C, which closely correlates with the DSC thermal event. The correlation between DSC and HSM provides strong evidence that the product is a well-defined cocrystal rather than an unreacted mixture. The thermal behavior of the synthesized cocrystal is shown in Figure 2, along with its DSC peaks and HSM images.

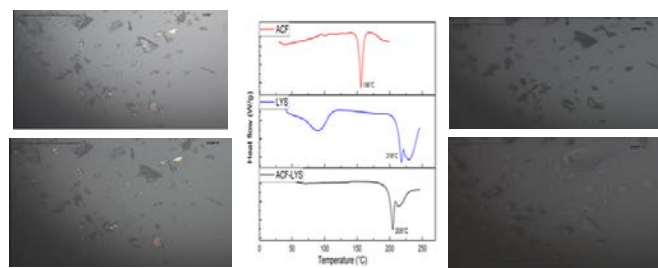


**Figure 2: DSC and Hot Stage Microscopy depicting thermal behaviour of ACF-LYS cocrystal**

### FTIR spectroscopy

FTIR spectroscopy was employed to investigate the molecular interactions responsible for cocrystal formation between ACF and LYS. Pure LYS displayed characteristic absorption peaks at 2931, 2863, 2132, 1587, and 1515 cm<sup>-1</sup>, while ACF exhibited distinct bands corresponding to its functional groups, such as the

C=O stretch ( $1767\text{ cm}^{-1}$ ), C–O stretching ( $1250\text{ cm}^{-1}$ ), O–H bending ( $1500\text{ cm}^{-1}$ ), and C–C stretching ( $1579\text{ cm}^{-1}$ ). These spectral features confirmed the presence of carboxylic and keto functionalities within the ACF structure [28, 29]. In the case of the ACF–LYS cocrystal, the IR spectrum revealed new absorption bands ( $3360.76, 3015.20, 2946.82, 1736.52, 1639.60, 1577.41, 1411.24, 1236.11, 1090.17, 770.47\text{ cm}^{-1}$ ), along with noticeable shifts, disappearance, or overlapping of ACF- and

LYS-specific peaks, as shown in **Table 3**. Such spectral modifications indicate altered hydrogen-bonding environments and molecular interactions between the drug and the coformer. The shift of the C=O stretching vibration (from  $1767\text{ cm}^{-1}$  to  $1739\text{ cm}^{-1}$ ) and changes in the N–H and O–H stretching regions provide strong evidence of hydrogen bond formation between ACF and LYS functional groups.

**Table 3: FTIR Spectrum of ACF: LYS Cocrystal**

Wavenumber ( $\text{cm}^{-1}$ )	Functional Group	Type of Vibration	Notes
3360.76	N-H (Amine, L-Lysine)	Stretch	Broad absorption may overlap with the O-H stretch
3015.20, 2946.82	O-H (Carboxylic Acid or Hydroxyl)	Stretch	Broad peak represents hydrogen bonding in the cocrystal.
1736.52	C=O (Carboxylic Acid & Ketone)	Stretch	Sharp peak, may shift due to Cocrystal formation
1639.60	C=C (Aromatic Ring)	Stretch	Characteristics of aromatic rings from Aceclofenac
1236.11	C-N (Amine)	Stretch	Peaks for the amine group in L-Lysine
770.47	C-Cl (Aryl Chloride)	Stretch	Characteristic of aryl chloride in Aceclofenac

These FTIR observations, when considered in conjunction with thermal analysis, confirm that the interaction between ACF and LYS has resulted in the formation of a new crystalline entity, rather than a simple physical mixture [20]. The FTIR overlay spectra of ACF, ACF LYS, and LYS are shown in **Figure 3**.

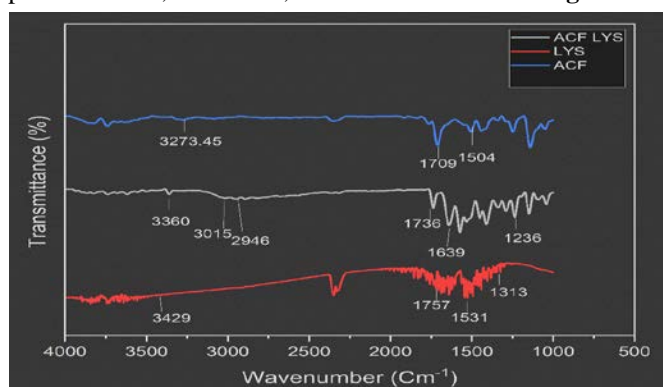


**Figure 3: FTIR Overlay Spectra of ACF, ACF-LYS, LYS**

### PXRD

The PXRD analysis clearly confirmed the formation of a new crystalline phase distinct from the parent drug and coformer. Pure aceclofenac (ACF) exhibited characteristic diffraction peaks at  $8.89^\circ, 11.64^\circ, 12.30^\circ, 14.60^\circ, 16.94^\circ, 18.65^\circ, 19.53^\circ, 22.38^\circ, 23.43^\circ, 26.49^\circ,$  and  $32.23^\circ$ , while L-lysine displayed major reflections at  $6.90^\circ, 10.23^\circ, 15.41^\circ, 18.64^\circ, 19.64^\circ, 20.59^\circ, 21.15^\circ, 23.72^\circ, 25.77^\circ, 27.06^\circ, 30.98^\circ,$  and  $32.96^\circ$ . In contrast, the PXRD diffractogram of the ACF–LYS cocrystal demonstrated several new peaks, most prominently at  $9.99^\circ, 10.03^\circ, 11.86^\circ, 17.29^\circ, 20.49^\circ, 21.08^\circ, 21.84^\circ, 22.63^\circ, 25.90^\circ, 26.30^\circ, 28.21^\circ, 33.36^\circ,$  and  $36.59^\circ$ . The emergence of these new

diffraction peaks, together with the merging of overlapping peaks (e.g., ACF  $18.40^\circ$  and LYS  $18.33^\circ$  merging at  $18.39^\circ$ , and ACF  $20.48^\circ$  with LYS  $20.80^\circ$  merging at  $20.61^\circ$ ), strongly indicates the generation of a new crystalline phase.

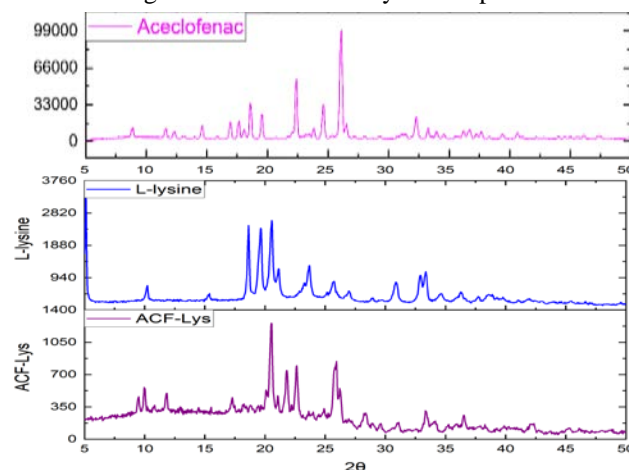


**Figure 4: The PXRD patterns of ACF pure drug, LYS coformer, and ACF-LYS cocrystal**

The simultaneous appearance of new reflections and modification of parent peaks rules out the possibility of a simple physical mixture, where the diffractogram would merely represent the superimposed patterns of ACF and LYS. Instead, the observed changes reflect a complete reorganization of the crystal lattice mediated by intermolecular interactions between the drug and the coformer. The percentage crystallinity of the synthesized cocrystal was found to be 95.7% by using the crystallinity formula:  $\% \text{ Crystallinity } (X_c) = (1 - A_{\text{amorphous}} / A_{\text{total}}) \times 100$ . Therefore, PXRD unambiguously confirms the

formation of the ACF–LYS cocrystal as a novel crystalline phase [30, 31]. The individual peaks of ACF, LYS, and ACF–LYS were shown in **Figure 4**.

### Dissolution Studies

The drug release study of ACF, ACF-LYS cocrystal, the physical mixture of ACF and LYS, and the marketed formulation was conducted in phosphate buffer at pH 7.5. Results demonstrated that the cocrystals exhibited improved solubility compared to the pure drug, the physical mixture, and the commercial product. Notably, the physical mixture showed a higher release rate than the pure drug alone, indicating some degree of interaction between the drug and coformer. The pure drug exhibited 6.69%, 11.56%, 16.60%, 21.81%, 24.21%, 27.89%, and 34.41%, and the physical mixture shows approximately 10.32%, 14.16%, 19.29%, 23.17%, 29.19%, 33.92% and 41.23%. ACF cocrystal exhibited a release of 21.02%, 42.22%, 65.10%, 83.40%, 90.92%, 91.49%, and 91.84%, while ACF marketed drug exhibited 23.66%, 45.59%, 65.65%, 77.58%, 84.88%, 86.69%, and 87.58% release respectively over different intervals 5, 10, 15, 30, 45, 60 and 90 minutes as shown in **Figure 5** [32]. The superior dissolution profile of the ACF–LYS cocrystal ( $p < 0.001$ ) confirms that cocrystallization is an effective strategy to overcome the solubility limitations of ACF, as the modified crystal lattice leads to

favourable molecular packing and hydrogen bonding that improve aqueous solubility and drug release behaviour.

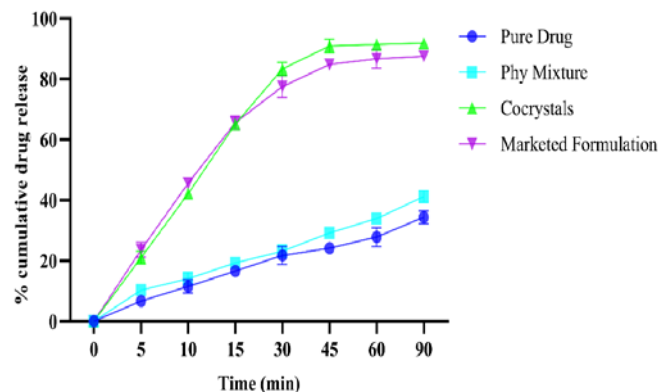


**Figure 5:** *In vitro* drug release of ACF, ACF cc, ACF PM, and MKT formulation

In zero-order kinetics, the drug is released at a constant rate over time, independent of its concentration. A linear relationship is observed when plotting the percentage of cumulative drug release versus time. For the **pure drug**, the zero-order plot yielded an **R<sup>2</sup> value**, suggesting a moderate fit and partial adherence to zero-order kinetics. For the **cocrystal**, the R<sup>2</sup> value is not suitable for a zero-order fit. This indicates the drug release is not constant and does not follow zero-order kinetics. First-order kinetics suggest that the rate of drug release is proportional to the amount of drug remaining.

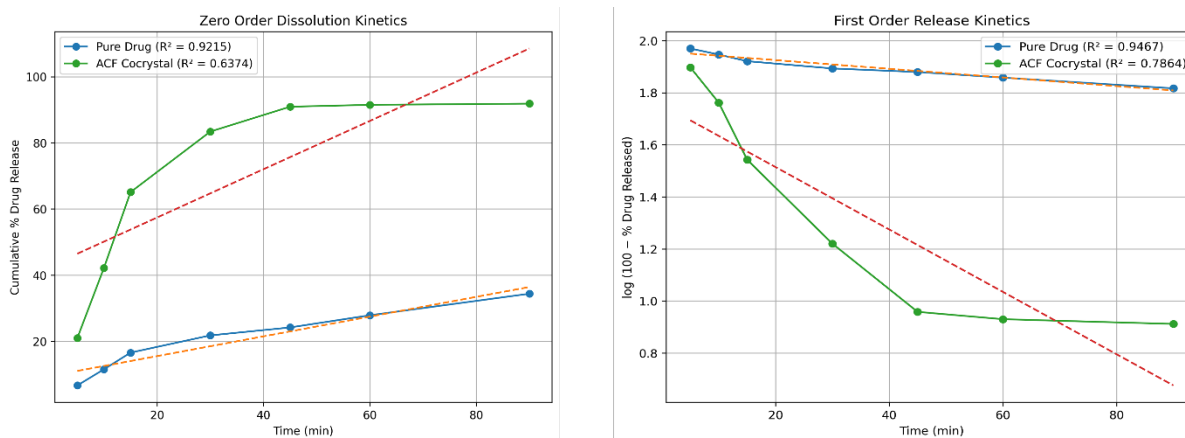


**Figure 6:** The Drug Kinetic Release over Time Zero order and First order Kinetics

A linear plot of  $\log (\% \text{ drug remaining})$  versus time is expected. For the **pure drug**, the first-order model provided a better fit ( $R^2$ ), suggesting that first-order kinetics more accurately describe its release behavior. For the **cocrystal**, the **R<sup>2</sup> value** indicates a good fit for the first-order kinetics. Kinetic modeling revealed that both pure ACF and the cocrystal follow first-order release kinetics ( $R^2 = 0.92$  and  $0.94$ , respectively), indicating concentration-dependent dissolution, where the release rate is

proportional to the amount of undissolved drug. The superior first-order fit confirms that dissolution is controlled by surface concentration gradients rather than by constant erosion, thereby validating that the cocrystal's enhanced wettability and reduced lattice energy drive the observed 2.67-fold increase in dissolution at 90 minutes and, ultimately, the 1.22-fold increase in therapeutic efficacy. The resulting drug kinetic release data are shown in **Figure 6**.

### Stability Studies

The stability of pure aceclofenac (ACF) and the aceclofenac–lysine (ACF–LYS) cocrystal was assessed under accelerated storage conditions (30 °C/65% RH and 40 °C/75% RH) for 6 months, following ICH Q1A(R2) guidelines. Both samples showed minor reductions in assay values over time; however, drug content consistently remained within the official acceptance criteria of 95–105%, confirming that neither formulation underwent significant chemical degradation. Although assay values were comparable, the key difference was observed in dissolution performance. Pure ACF showed limited release (approximately 34% at 90 min initially, declining to approximately 30% after 6 months at 40 °C/75% RH), reflecting its inherent solubility challenges and susceptibility to performance degradation during storage. In contrast, the ACF–

LYS cocrystal exhibited a markedly higher release profile (≈approximately 92% at 90 min initially, remaining above 86% after 6 months at 40 °C/75% RH), as shown in **Table 4**.

The dissolution advantage was preserved across all time points and storage conditions, indicating that the cocrystal structure remained intact and functionally stable throughout the study period [32]. These findings confirm that cocrystallization not only enhances the solubility and dissolution of ACF but also produces a formulation with satisfactory stability under accelerated conditions. The ability of the ACF–LYS cocrystal to sustain its dissolution benefit despite exposure to stress conditions underscores its potential as a superior alternative to conventional ACF formulations for improving therapeutic performance (ICH, 2003) [32].

**Table 4: Stability Studies of Aceclofenac Cocrystal**

Sample	Test name	Initial	30°C/65% RH			40°C/75% RH		
			1M	3M	6M	1M	3M	6M
Aceclofenac	Description	White	White	White	White	White	White	White
	Assay	99.961	99.160	98.298	97.543	98.187	97.590	96.309
	Dissolution							
	0 min	0	0	0	0	0	0	0
	30 min	21.818	21.546	21.408	20.815	21.135	20.345	19.678
	60 min	27.896	27.775	26.876	25.386	27.076	25.309	23.659
	90 min	34.410	33.874	33.089	32.238	33.409	31.537	30.169
Cocrystals	Description	Pale white	Pale white	Pale white	Pale white	Pale white	Pale white	Pale white
	Assay	99.85	99.328	98.502	97.091	99.087	97.659	96.033
	Dissolution							
	0 min	0	0	0	0	0	0	0
	30 min	83.407	82.832	81.187	80.872	83.123	82.332	80.117
	60 min	91.490	90.409	89.023	87.824	90.209	88.708	86.554
	90 min	91.846	90.505	89.823	87.297	90.976	87.465	86.743

### Anti-inflammatory activity

The anti-inflammatory efficacy of the aceclofenac–lysine (ACF–LYS) cocrystal was evaluated using the carrageenan-induced paw edema model in rats. Pure aceclofenac produced a moderate anti-inflammatory effect, with percentage inhibition values ranging from 27.39% at 1 hour to 74.35% at 5 hours. In contrast, animals treated with the ACF–LYS cocrystal exhibited consistently higher inhibition of edema, ranging from 34.79% at 1 hour to 81.50% at 5 hours. The change in paw volume over time for different groups is depicted in Figure 7, while the corresponding percentage inhibition with error bars is presented in Figure 8. The greater inhibition observed with the cocrystal

than with the pure drug at every time point indicates improved therapeutic efficacy. This enhanced activity may be attributed to improved solubility and dissolution of the cocrystal, which likely led to better systemic drug availability [33]. The cocrystal's 2.67-fold increase in dissolution rate was strongly correlated with a 1.22-fold improvement in anti-inflammatory efficacy ( $p < 0.05$ ). Mechanistically, reduced lattice energy ( $\Delta H_f$ : -11.4%) drives rapid dissolution (83.4% at 30 min vs 21.8% for pure ACF), generating supersaturation that increases intestinal absorption and systemic bioavailability. The enhanced dissolution behavior is presumed to facilitate rapid and efficient drug absorption, thereby increasing systemic bioavailability and

a pronounced pharmacodynamic response. Similar correlations between dissolution enhancement and therapeutic efficacy have been reported for other aceclofenac cocrystals, where improved solubility has directly contributed to superior bioavailability and overall pharmacological performance.

Statistical analysis using one-way ANOVA further confirmed the significance of these findings ( $p < 0.0001$ ), and the F-statistic [ $F = 10.5$ ,  $p < 0.0001$ ], specific post-hoc test used (Tukey's multiple comparison test), and exact p-values for all pairwise comparisons, particularly the critical comparison between cocrystal and pure aceclofenac ( $p < 0.0001$ ), demonstrating that the cocrystal was more effective in reducing inflammation compared with both the control and pure drug groups. These results suggest that the improved physicochemical properties of the cocrystal, demonstrated in earlier *in vitro* studies, directly translated into enhanced pharmacological performance *in vivo*. Overall, the ACF-LYS cocrystal not only retained the anti-inflammatory potential of aceclofenac but also enhanced its efficacy, underscoring the potential of cocrystallization as a formulation strategy to improve therapeutic outcomes [33].

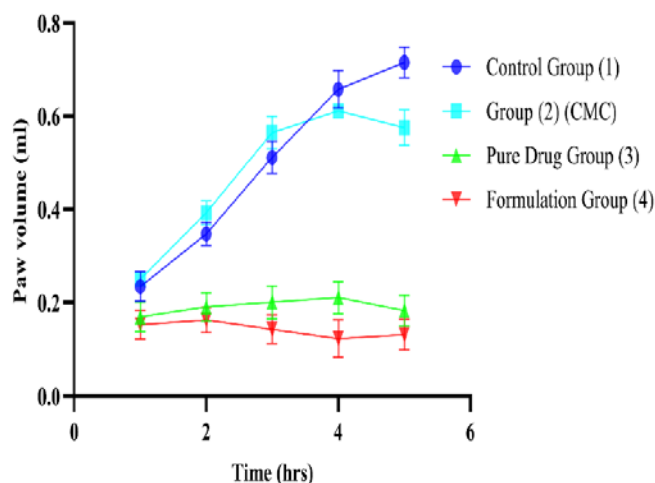


**Figure 7: Anti-inflammatory activity in Wistar rats in Group 1 (Control), Group 2 (CMC), Group 3 (Pure drug), Group 4 (Formulation)**

## DISCUSSION

This study demonstrated the development of Aceclofenac cocrystals with GRAS-listed coformers, in which lysine was identified as the most favorable partner based on molecular electrostatic potential (MESP) analysis and DFT calculations. The computed interaction energy ( $\Delta E = 37.6$  kJ/mol) and the strong electrostatic compatibility between the carboxyl group of aceclofenac and the  $\text{NH}_3^+/\text{COO}^-$  groups of lysine suggest the

formation of stable supramolecular structures. This result aligns with previous studies showing that  $\Delta E$  values exceeding 11 kJ/mol indicate a strong potential for cocrystal formation. The negative interaction energies predicted by DFT support the formation of stable supramolecular assemblies, in line with previous computational studies on cocrystal screening, which have shown that hydrogen-bond complementarity can be reliably predicted through electrostatic potential mapping [34].

The neat grinding method not only aligns with green chemistry principles by eliminating solvent use. Three batches of aceclofenac-lysine co-crystals were synthesized using the neat grinding method with identical stoichiometric ratios 1:1 (708.378 mg aceclofenac and 292.380 mg L-lysine per batch). The synthesis demonstrated excellent reproducibility, with a mean yield of  $98.21 \pm 0.31\%$  ( $n = 3$ ,  $\text{RSD} = 0.32\%$ ), indicating reliable and efficient co-crystal formation suitable for pharmaceutical development and scale-up. PXRD analysis demonstrating consistent diffraction patterns with characteristic peaks at  $9.99^\circ$ ,  $10.03^\circ$ ,  $11.86^\circ$ ,  $17.29^\circ$ ,  $20.49^\circ$ , and  $21.08^\circ$  ( $2\theta$ ). Relative standard deviation (RSD) for major peak intensities was  $< 5\%$ , confirming excellent batch-to-batch reproducibility. Further experiments, characterized by using FTIR, DSC, and HSM, confirmed the formation of a novel crystalline phase distinct from the parent components.

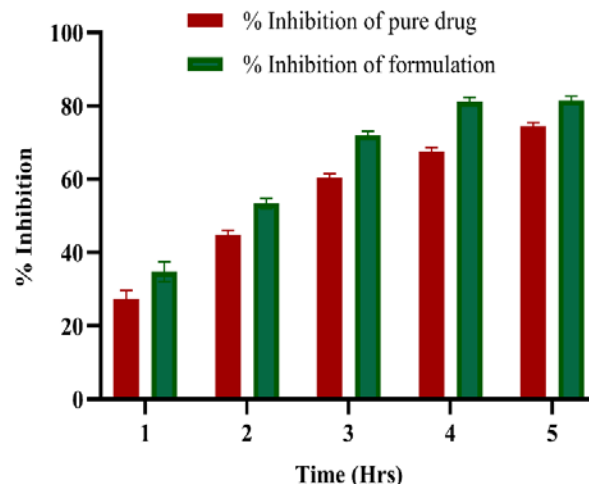


**Figure 8: % Inhibition activity in Wistar rat (Pure drug and Formulation)**

The shift of the C=O stretching vibration (from  $1767\text{ cm}^{-1}$  to  $1739\text{ cm}^{-1}$ ) and changes in the N-H and O-H stretching regions provide strong evidence of hydrogen bond formation between ACF and LYS functional groups. The synthesized ACF-LYS cocrystal displayed a distinctive melting endotherm at  $205^\circ\text{C}$ ,

positioned between the melting points of the two parent components. The Hot-stage microscopy (HSM) observations supported these findings: the cocrystal began to melt at 203.6 °C and completely melted at 206.8 °C, which closely correlates with the DSC thermal event. The disappearance of individual melting peaks in DSC thermograms and the emergence of new PXRD peaks indicate successful cocrystallization. Similar thermal and spectroscopic transformations have been reported for other Aceclofenac cocrystals, such as Aceclofenac–dimethylurea [35] and Aceclofenac–nicotinamide [36], where characteristic shifts in FTIR spectra and disappearance of parent drug peaks confirmed the establishment of new supramolecular arrangements.

The cocrystal with lysine exhibited enhanced dissolution in phosphate buffer (pH 7.5) relative to the pure drug, the physical mixture, and the marketed formulation. The aceclofenac–lysine cocrystal showed a 2.66-fold higher dissolution rate in phosphate buffer (pH 7.5) than pure aceclofenac and a 1.04-fold increase compared to the marketed formulation. This improvement is likely due to ionic and hydrogen-bond interactions within the cocrystal lattice, which enhance wettability and lower the dissolution energy barrier [35, 39]. Similarly, solid dispersion systems of Aceclofenac with HPMC [37] and hydrotropic solubilization methods [38] also yielded enhanced dissolution rates, supporting the role of supramolecular modifications in improving biopharmaceutical performance.

The improved dissolution characteristics of aceclofenac are attributable to several underlying mechanisms, including the lysine cocrystal. Primarily, the formation of hydrogen-bonded supramolecular networks between the carboxylic acid moiety of aceclofenac and the amino and carboxyl groups of lysine lowers the lattice energy, producing a less compact crystal lattice that dissociates more readily in aqueous environment. Moreover, the hydrophilic properties of lysine enhance surface wettability, promoting faster diffusion of the dissolution medium and subsequent drug release. The grinding process also generates smaller particles with a larger surface area, thereby further enhancing dissolution. Together, these factors—reduced lattice stability, improved wettability, and optimized particle morphology—account for the increased solubility and dissolution rate. This accelerated dissolution likely translates into improved drug absorption and superior *in vivo* anti-

inflammatory activity. Anti-inflammatory efficacy, evaluated using a carrageenan-induced paw edema model, revealed that the cocrystal formulations produced a more pronounced inhibitory effect than the pure drug. Cocrystal formulation exhibits greater efficacy in reducing inflammation. The *in vivo* anti-inflammatory activity, assessed using the carrageenan-induced paw edema test, showed that the cocrystal produced 81.50% edema inhibition after 5 hours, compared with 74.35% for the pure drug ( $p < 0.0001$ ), indicating superior therapeutic efficacy. The improved bioavailability correlates with faster dissolution and better solubilization, linking physicochemical changes to enhanced pharmacodynamic outcomes [33].

Finally, stability studies revealed that the Aceclofenac–lysine cocrystal met official criteria (95–105%) under accelerated conditions for up to six months, although some degradation was observed during extended storage. Comparable results were reported by Patil et al. (2021), where Aceclofenac–DMU cocrystals remained stable for three months under ICH conditions. Overall, these comparisons demonstrate that lysine-based Aceclofenac cocrystals improve dissolution and anti-inflammatory efficacy, as well as stability over time [35].

## CONCLUSION

This research work has effectively established the synthesis and thorough evaluation of aceclofenac Lysine cocrystals as a viable solution for enhancing the poor aqueous solubility characteristics inherent to this BCS Class II pharmaceutical compound. Cocrystal formation was substantiated through a battery of analytical methods, whereby XRD analysis exhibited unique crystalline patterns reflecting novel solid-state arrangements, hot stage microscopy showed distinctive thermal transitions, differential scanning calorimetry indicated modified phase behavior in the thermograph, and infrared spectroscopy verified the presence of hydrogen bond networks between the drug molecule and the cocrystal former. *In vitro* solubility assessments demonstrated marked improvements in dissolution performance and aqueous solubility for the prepared cocrystal L-lysine systems, when benchmarked against the API aceclofenac, thereby effectively addressing the compound's fundamental bioavailability constraints.

Long-term stability evaluations established that the engineered cocrystals retained their superior dissolution characteristics across different environmental conditions, confirming their

suitability for pharmaceutical development. Crucially, *in vivo* studies in paw oedema models confirmed the therapeutic benefits of enhanced dissolution, with cocrystal preparations of ACF-L-lysine exhibiting improved anti-inflammatory responses compared with conventional aceclofenac formulations.

The cumulative evidence supports cocrystal engineering as a valuable pharmaceutical strategy for optimizing aceclofenac's biopharmaceutical profile, potentially translating to better clinical outcomes through enhanced drug absorption and pharmacological activity. The multifaceted analytical methodology employed in this investigation provides a solid foundation for subsequent cocrystal research. It represents a meaningful contribution to the field of pharmaceutical solid-state chemistry.

Although the current work is limited to laboratory and animal studies, the results provide a strong basis for future pharmacokinetic and clinical investigations. In the current pharmaceutical landscape, where enhancing solubility remains a key challenge, this research highlights cocrystal engineering as a practical and efficient strategy to improve drug performance. Overall, this work provides valuable insights into solid-state drug development and supports continued exploration of cocrystals to enhance therapeutic outcomes.

#### ABBREVIATIONS:

ACF – Aceclofenac; LYS – Lysine; BCS – Biopharmaceutical Classification System; API – Active Pharmaceutical Ingredient XRD – Powder X-ray Diffraction; USFDA – U.S. Food and Drug Administration; NSAIDs – Non-Steroidal Anti-Inflammatory Drugs; FTIR – Fourier Transform Infra-red Spectroscopy; HSM – Hot Stage Microscopy; DSC – Differential Scanning Calorimetry; USP – United States Pharmacopeia

#### FINANCIAL ASSISTANCE

NIL

#### CONFLICT OF INTEREST

The authors declare no conflict of interest.

#### AUTHOR CONTRIBUTION

Aditay Kumar contributed to the conceptualization, methodology, investigation, data curation, writing the original draft, writing the review, and editing. Mahesh Kumar

contributed to the supervision, methodology, resources, writing review, and editing. All authors read and approved the final manuscript to be published. This research was conducted manually in a laboratory, without the involvement of a paper mill or artificial intelligence.

#### REFERENCES

- [1] Iolascon G, Gimenez S, Mogyrosi D. A review of aceclofenac: analgesic and anti-inflammatory effects on musculoskeletal disorders. *J. Pain Res.*, **14**, 3651–63 (2021) <https://doi.org/10.2147/JPR.S326101>
- [2] Jessica A, Wahyuni SN, Zaini E, Fitriani L. Increased dissolution rate of aceclofenac by formation of multicomponent crystals with L-glutamine. *Int. J. Appl. Pharm.*, **16**(S1), 45–52 (2024) <https://doi.org/10.22159/ijap.2024.v16s1.09>
- [3] Shakeel F, Al-Shdefat R, Altamimi MA, et al. Solubility and thermodynamic analysis of aceclofenac in different {Carbitol + water} mixtures at various temperatures. *BMC Chem.*, **18**, 168 (2024) <https://doi.org/10.1186/s13065-024-01287-z>
- [4] Kumar A, Kumar M. Improvisation of dissolution profile of aceclofenac by using cocrystallization technique. *Afr. J. Biomed. Res.*, **27**(4S), 11518–24 (2024) <https://doi.org/10.53555/AJBR.v27i4S.5769>
- [5] Tran P, Pyo YC, Kim DH, Lee SE, Kim JK, Park JS. Overview of the manufacturing methods of solid dispersion technology for improving the solubility of poorly water-soluble drugs and application to anticancer drugs. *Pharmaceutics*, **11**(3), 132 (2019) <https://doi.org/10.3390/pharmaceutics11030132>
- [6] Luke DR, Tomaszewski K, Damle B, Schlamm HT. Review of the basic and clinical pharmacology of sulfobutylether- $\beta$ -cyclodextrin (SBECD). *J. Pharm. Sci.*, **99**(8), 3291–301 (2010) <https://doi.org/10.1002/jps.22109>
- [7] Nurismi E, Rosaini H. Effect of different methods on the multicomponent crystal formation from medicinal natural ingredient compounds. *Int. J. Pharm. Sci. Med.*, **6**(5), 32–9 (2021) <https://doi.org/10.47760/ijpsm.2021.v06i05.004>
- [8] Kumar S, Gupta A, Prasad R, Singh S. Novel aceclofenac cocrystals with L-cystine: virtual cofomer screening, mechanochemical synthesis, and physicochemical investigations. *Curr. Drug Deliv.*, **18**(1), 88–100 (2021) <https://doi.org/10.2174/1567201817666200817110949>
- [9] Sharma S, Kumar S, Gupta A, et al. Screening of aceclofenac for cocrystallization with nicotinamide: theoretical and practical perspective. *Indian J. Pharm. Sci.*, **84**(6), 1396–1405 (2022) <https://doi.org/10.36468/pharmaceutical-sciences.1396>
- [10] Yousef MA, Vangala VR. Pharmaceutical cocrystals: molecules, crystals, formulations, medicines. *Cryst. Growth Des.*, **19**(12), 7420–38 (2019) <https://doi.org/10.1021/acs.cgd.8b01898>
- [11] Grothe E, Meekes H, Vlieg E, ter Horst JH, de Gelder R. Solvates, salts, and cocrystals: a proposal for a feasible

- classification system. *Cryst. Growth Des.*, **16**(6), 3237–43 (2016) <https://doi.org/10.1021/acs.cgd.6b00200>
- [12] Kumar S, Nanda A. Pharmaceutical cocrystals: an overview. *Indian J. Pharm. Sci.*, **79**(6), 858–71 (2017) <https://doi.org/10.4172/pharmaceutical-sciences.1000302>
- [13] Bolla G, Sarma B, Nangia AK. Crystal engineering of pharmaceutical cocrystals in the discovery and development of improved drugs. *Chem. Rev.*, **122**(13), 11514–603 (2022) <https://doi.org/10.1021/acs.chemrev.1c00987>
- [14] Putri D. Review: multicomponent crystals: cinnamic acid as a co-former. *Int. J. Pharm. Sci. Med.*, **6**(1), 92–8 (2021) <https://doi.org/10.47760/ijpsm.2021.v06i01.008>
- [15] Afzal H, Abbas N, Hussain A, Latif S, Fatima K, Arshad MS. Physicomechanical, stability, and pharmacokinetic evaluation of aceclofenac dimethyl urea cocrystals. *AAPS PharmSciTech*, **22**(2), 68 (2021) <https://doi.org/10.1208/s12249-021-01938-7>
- [16] Sharma G, Saini MK, Thakur K, Kapil N, Garg NK, Raza K. Aceclofenac cocrystal nanoliposomes for rheumatoid arthritis with better dermatokinetic attributes: a preclinical study. *Nanomedicine*, **12**(6), 615–38 (2017) <https://doi.org/10.2217/nnm-2016-0405>
- [17] Kumar S, Gupta A, Prasad R, Singh S. Novel aceclofenac cocrystals with L-cystine: virtual cofomer screening, mechanochemical synthesis, and physicochemical investigations. *Curr. Drug Deliv.*, **18**(1), 88–100 (2021) <https://doi.org/10.2174/1567201817666200817110949>
- [18] Sohrab M, Mahapatra SP, Tiwari S. Enhancement of dissolution rate of aceclofenac by formation of aceclofenac–nicotinic acid cocrystal using water-soluble polymers like PVP K-30, HPMC E5, SSG, and Na-CMC. *Indo Glob. J. Pharm. Sci.*, **5**(3), 154–70 (2015) <https://doi.org/10.35652/IGJPS.2015.01>
- [19] Molajafari F, Li T, Abbaschaleshtori M, et al. Computational screening for prediction of co-crystals: method comparison and experimental validation. *CrystEngComm*, **26**, 1620–36 (2024) <https://doi.org/10.1039/D3CE01252B>
- [20] Neese F. The ORCA program system. *Wiley Interdiscip. Rev. Comput. Mol. Sci.*, **2**(1), 73–8 (2012) <https://doi.org/10.1002/wcms.81>
- [21] Neese F. Software update: the ORCA program system, version 4.0. *Wiley Interdiscip. Rev. Comput. Mol. Sci.*, **8**(1), e1327 (2018) <https://doi.org/10.1002/wcms.1327>
- [22] Lu T, Chen F. Multiwfn: a multifunctional wavefunction analyzer. *J. Comput. Chem.*, **33**(5), 580–92 (2012) <https://doi.org/10.1002/jcc.22885>
- [23] Zhang H, Zeng H, Li M, Song Y, Tian S, Xiong J, et al. Novel ascorbic acid co-crystal formulations for improved stability. *Molecules*, **27**(22), 7998 (2022) <https://doi.org/10.3390/molecules27227998>
- [24] Kumar A, Nanda A. Similar but not same: impact of structurally similar cofomers on co-crystallization with telmisartan. *J. Pharm. Innov.*, **18**(4), 1954–65 (2023) <https://doi.org/10.1007/s12247-023-09759-w>
- [25] Alenazi NA, Bokhari MG, Abourehab MAS, Abukhadra MR, El-Gendy EM, El-Sayed YM, et al. Drug polymeric carrier of aceclofenac based on amphiphilic chitosan micelles. *ACS Omega*, **8**(50), 48145–58 (2023) <https://doi.org/10.1021/acsomega.3c07065>
- [26] Weng J, Wong SN, Xu X, Xuan B, Wang C, Chen R, et al. Cocrystal engineering of itraconazole with suberic acid via rotary evaporation and spray drying. *Cryst. Growth Des.*, **19**(5), 2736–45 (2019) <https://doi.org/10.1021/acs.cgd.8b01873>
- [27] Haneef J, Chadha R. Drug–drug multicomponent solid forms: cocrystal, coamorphous and eutectic of three poorly soluble antihypertensive drugs using a mechanochemical approach. *AAPS PharmSciTech*, **18**, 2279–90 (2017) <https://doi.org/10.1208/s12249-016-0701-1>
- [28] Adhitya J, Wahyuni NY, Zaini E, Fitriani L. Increased dissolution rate of aceclofenac by formation of multicomponent crystals with L-glutamine. *Int. J. Appl. Pharm.*, **16**(1), 45–52 (2024) <https://doi.org/10.22159/ijap.2024.v16s1.09>
- [29] Rupal J, Kaushal J, Mallikarjuna SC, Dipti P. Preparation and evaluation of solid dispersions of aceclofenac. *Int. J. Pharm. Sci.*, **1**(1), 32–5 (2009) <https://doi.org/10.25004/IJPSDR.2009.010108>
- [30] Lapidus SH, Stephens PW, Arora KK, Shattock TR, Zaworotko MJ. A comparison of cocrystal structure solutions from powder and single crystal techniques. *Cryst. Growth Des.*, **10**, 4630–7 (2010) <https://doi.org/10.1021/cg1009237>
- [31] Kavuru P, Aboarayas D, Arora KK, Clarke HD, Kennedy A, Marshall L, et al. Hierarchy of supramolecular synthons: persistent hydrogen bonds between carboxylates and weakly acidic hydroxyl moieties in cocrystals of zwitterions. *Cryst. Growth Des.*, **10**, 3568–84 (2010) <https://doi.org/10.1021/cg100565a>
- [32] Afzal H, Abbas N, Hussain A, Latif S, Fatima K, Arshad MS, et al. Physicomechanical, stability, and pharmacokinetic evaluation of aceclofenac–dimethyl urea cocrystals. *AAPS PharmSciTech*, **22**(2), 68 (2021) <https://doi.org/10.1208/s12249-021-01938-7>
- [33] Usha AN, Mutalik S, Reddy MS, Ranjith AK, Kushtagi P, Udupa N. Preparation and in vitro, preclinical and clinical studies of aceclofenac spherical agglomerates. *Eur. J. Pharm. Biopharm.*, **70**(2), 674–83 (2008) <https://doi.org/10.1016/j.ejpb.2008.06.010>
- [34] Ahmadi S, Mondal PK, Wu Y, Gong W, Mirmehrabi M, Rohani S. Virtual multicomponent crystal screening: hydrogen bonding revisited. *Cryst. Growth Des.*, **21**(10), 5862–72 (2021) <https://doi.org/10.1021/acs.cgd.1c00737>
- [35] Patil SP, Kulkarni AS, Patel SK, Dave RH. Physicomechanical and stability evaluation of aceclofenac–dimethylurea cocrystals. *AAPS PharmSciTech*, **22**(3), 93 (2021) <https://doi.org/10.1208/s12249-021-01938-7>

- [36] Shete AS, Yadav AV, Doijad RC. Screening of aceclofenac for cocrystallization with nicotinamide: theoretical and practical perspective. *Indian J. Pharm. Sci.*, **84(6)**, 1389–97 (2022) <https://doi.org/10.36468/pharmaceutical-sciences.1037>
- [37] Rusli D, Umar S, Aldi Y, Usman H, Siregar MN, Zaini E. Enhancement of aceclofenac dissolution rate via solid dispersion with hydroxypropyl methylcellulose. *Trop. J. Nat. Prod. Res.*, **9(1)**, 152–6 (2025) <https://doi.org/10.26538/tjnpr/v9i1.22>
- [38] Sarkar P, Biswas M. Formulation development and in vitro characterization of ternary hydrotropic solid dispersions of aceclofenac. *Asian J. Pharm. Clin. Res.*, **15(9)**, 174–9 (2022) <https://doi.org/10.22159/ajpcr.2022.v15i9.45158>
- [39] Kumar A, Kumar M. Improvisation of dissolution profile of aceclofenac by using cocrystallization technique. *Afr. J. Biomed. Res.*, **27(4S)**, 11518–24 (2024) <https://doi.org/10.53555/AJBR.v27i4S.5769>